PV Cell Angle Optimisation for Energy Arrival-Consumption Matching in a Solar Energy Harvesting Cellular Network

Doris Benda*, Xiaoli Chu*, Sumei Sun†, Tony Q.S. Quek‡ and Alastair Buckley*
* University of Sheffield, United Kingdom
† Institute for Infocomm Research - A*Star, Singapore
‡ Singapore University of Technology and Design, Singapore
E-mail: dcbenda1@sheffield.ac.uk, x.chu@sheffield.ac.uk, sunsm@i2r.a-star.edu.sg,
tonyquek@sutd.edu.sg and alastair.buckley@sheffield.ac.uk

***Abstract*—Despite the increasing interest in photovoltaic (PV) cell powered small-cell base stations (SBSs), it has not been sufficiently studied yet how different PV cell angles can be utilized to achieve a good match between the energy arrival and consumption at the SBS. This is especially important in an urban environment where cellular network operators often struggle to apply optimal angles to the PV cells due to implementation constraints or shadowing effects of surrounding buildings. We develop an energy generation, storage and consumption model of a PV cell powered SBS, which includes the effects of PV cell orientations. A linear optimization problem is derived to optimize the energy performance of the SBS throughout the day. The effects of different PV cell orientations on the green energy utilization are evaluated assuming deployment in London in summer and winter. Our results show that west orientated PV cells (45° misalignment to the southern direction) are preferred in London during summer, whereas south orientated ones are preferred during winter. This reveals that the PV cell orientation needs to be optimized for not only the location and weather of the SBS deployment site but also the network traffic distribution in time (or energy consumption profile) of the deployment location.**

***Index Terms*—Green cellular network, solar cells, orientation angle, inclination angle and downlink transmission**

I. Introduction

A. Related Work

The information and communications technology (ICT) accounts for 3% of the global electricity costs with an increase rate of 15-20% every year [1]. Base stations are responsible for more than half of the energy costs in the cellular network infrastructure [2], indicating a huge demand to take advantage of renewable energy generation. Experts estimated that energy harvesting technology can reduce 20% of the CO_2 emissions in the ICT industry [3].

The next generation cellular network requires a massive expansion of the small-cell base station (SBS) deployment [4]. In contrast to the increased energy consumption for operating large numbers of SBSs, many countries have set green taxation and incentive schemes to achieve ambitious CO_2 emission reduction targets, making renewable energy harvesting technologies attractive for cellular network operators. Solar powered SBSs have been considered for future cellular networks due to their small physical footprint in dense built environments, technology maturity, low maintenance cost and production cost reduction in recent years [5].

Although cellular networks with solar harvesting SBSs have attracted significant interest recently, especially in the areas of combining wind and solar harvesting SBSs [6], dealing with the energy spatial [5] and temporal variations [7] of renewable energy, all these studies assumed optimally aligned PV cells (i.e., optimal orientation and inclination angles). To the best of our knowledge, there has not been any reported study considering a cellular network with a mixture of different aligned PV cells, which represents a more realistic urban cellular network.

B. Overview - Energy generation and consumption profiles

There exist an optimal PV cell orientation angle and an optimal PV cell inclination angle for a given geographical location of a SBS, which provide the highest average solar energy yield per day [8]. On the one hand, misaligned PV cells (i.e. with sub-optimal orientation and/or inclination angle) generate less solar energy in total. On the other hand, their daily solar energy profile can be shifted toward the morning or afternoon by adjusting the orientation angle (cf. Fig. 1 and Fig. 2), hence shifting the solar energy harvesting profile of the cellular network in the time domain. Locations close to the equator have an optimum inclination angle of around 0°, therefore their inclination angle has to be increased as well to make use of different orientation angles as a method to shift the solar energy harvesting profile in the time domain.

The energy consumption profile at a SBS is linked to the traffic load profile of the deployment area. For example, the highest energy consumption is expected at 23:00 and 11:30 am for residential areas and business areas, respectively [9].

978-1-4673-8999-0/17/$31.00 ©2017 IEEE

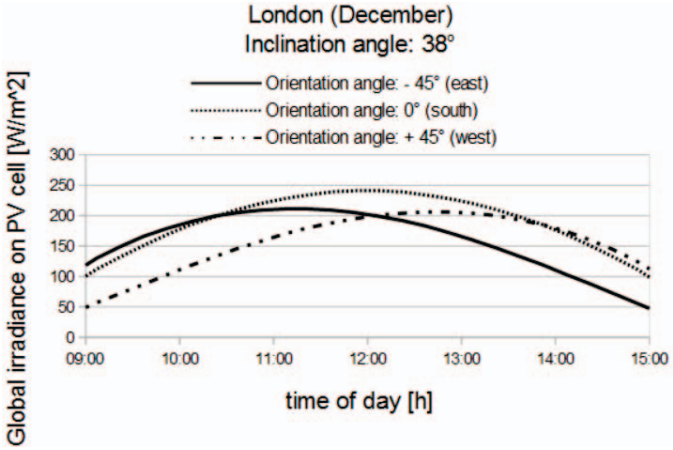

Fig. 1: Global irradiance comparison of different orientated PV cell installations in London in December. The optimum orientation (inclination) angle is 0° (38°) for London. Data source: [10]

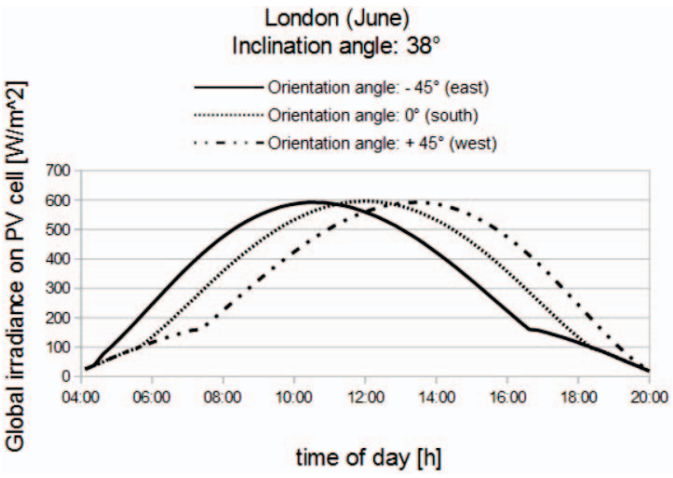

Fig. 2: Global irradiance comparison of different orientated PV cell installations in London in June. The optimum orientation (inclination) angle is 0° (38°) for London. Data source: [10]

C. Contributions and Organization

In this paper, we investigate how the PV cell orientation angles can be harnessed to achieve a good match between the energy arrival and consumption profiles at a PV cell powered SBS.

The contributions of the paper can be summarized as follows:

- We establish a system model and an analytical framework incorporating the effects of different inclination and orientation angles at a PV cell powered SBS.
- We evaluate the effects of different PV cell orientation angles on the green energy utilization of the SBS in different seasons based on a case study in London.
- We develop an algorithm to select the optimal PV cell orientation angle from a predefined set.

The rest of this paper is organized as follows. Section II presents a general energy generation, storage and consumption model of a PV cell powered SBS, which includes the effects of PV cell alignments. Section III derives a linear optimization problem to optimize the energy performance of the SBS throughout the day. Section IV presents and discusses the simulated numerical results based on a case study in London. Finally, the paper is concluded in Section V.

Notations: All matrices are denoted by bold capital letters, all vectors are denoted by bold lowercase letters, and an asterisk is added to the letter if it is an optimized matrix or vector.

II. System Models

A. SBSs Model

Each SBS has a coverage area radius of r_s and is completely powered by a PV cell with no main grid energy supply. A SBS becomes inactive if no user equipment (UE) is in its coverage area or when the SBS runs out of energy. If the SBS cannot serve its UEs, we assume that the UEs are offloaded to a different tier in the heterogeneous cellular network, e.g., a main grid connected macro base station (MBS). It is not in the scope of this paper to analyze the performance of this macro base station tier.

The inclination angle of a PV cell is defined as the angle between the horizontal plane and the PV cell panel. The orientation angle of a PV cell is defined as the angle between the southern direction and the projection of the line that points perpendicular out of the PV panel in the horizontal plane (cf. Fig. 3). Orientating the PV cell to the east (west) is indicated by a negative (positive) algebraic sign added to the orientation angle. The setups of all SBSs and PV panels are identical except that the inclination and/or orientation angles may vary among different SBSs. The index of a SBS is referred to as $k \in \{1, ..., K\}$, where K is the total number of SBSs. The orientation (inclination) angle of the k^{th} SBS is denoted as θ_k (γ_k). For example, the first SBS is depicted in Fig. 3 with $\theta_1 = -45°$ and $\gamma_1 = 38°$.

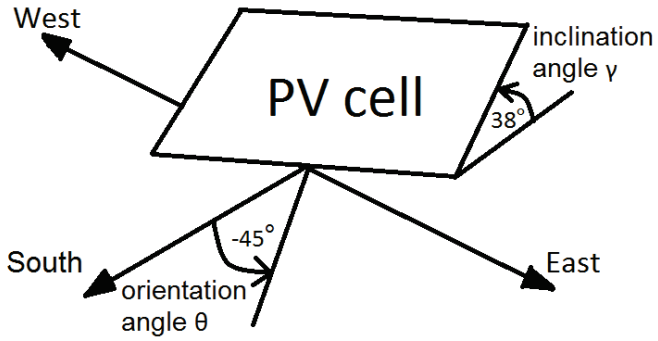

Fig. 3: Definition of the orientation angle θ and inclination angle γ of a PV cell

B. Solar Energy Harvesting Model

There are 4 astronomical events (equinox in March and September, solstice in June and December), which significantly affect the solar energy arrival in most geographical areas. Therefore, the solar energy harvesting model has to take these annual differences into account and be evaluated throughout the year to represent the different seasons accordingly.

A day is divided into T time steps. Denote t as the index of a time step, $t \in \{1, ..., T\}$. The energy harvesting profile of the SBS correlates with the solar irradiance. The harvested solar energy $a_k^{(t)}$ at the k^{th} SBS in the t^{th} time step is given by

$$a_k^{(t)} = G_k^{(t)} \cdot \eta \tag{1}$$

where $G_k^{(t)}[W/m^2]$ is the global irradiance value on the PV cell at the k^{th} SBS in the t^{th} time step [10], and η is the PV cell energy conversion efficiency coefficient.

The general daily irradiance value $G_k^{(t)}$ is derived from the data base [10], which provides data for any combination of orientation angle, inclination angle, month and location in Europe and Asia, with a 15-minute time resolution. The harvested solar energy in each time step can either be immediately consumed by the SBS or stored in a battery of capacity c_{max}.

C. Solar Energy Consumption Model and Traffic Load Model

The energy consumption of a SBS can be divided in a load independent part and a load dependent part. The load independent energy consumption is constant for different SBSs and time steps and is donated as e_{fix}. It includes the energy consumption of the baseline operations, such as transmitting signal beacons and circuit cooling operations. The load dependent energy consumption per time step increases with the number of UEs connected to the SBS due to the increased traffic load. Accordingly, the total energy consumption $e_k^{(t)}$ of the k^{th} SBS in the t^{th} time step is given by

$$e_k^{(t)} = e_{fix} + e_{user} \cdot l_k^{(t)} \tag{2}$$

where e_{fix} and $e_{user} \cdot l_k^{(t)}$ denote the load independent and load dependent energy consumption, respectively, whereas e_{user} is the average energy consumed by the SBS for serving one UE, and $l_k^{(t)}$ is the number of UE served by the k^{th} SBS in the t^{th} time step.

The total number of UE located in the coverage area of the k^{th} SBS in the t^{th} time step is calculated based on the downlink traffic distribution over time in a business district (cf. Fig. 4) as follows

$$l_k^{(t)} = round(user\_density(\lfloor t \rfloor_h) \cdot u_{max}) \quad \forall t \in \{1, ..., T\} \tag{3}$$

where the time step t is rounded down to the nearest full hour, $user\_density(\lfloor t \rfloor_h)$ is the user density at $\lfloor t \rfloor_h$ according to Fig. 4, and u_{max} is the maximum number of UEs in the coverage area of the SBS.

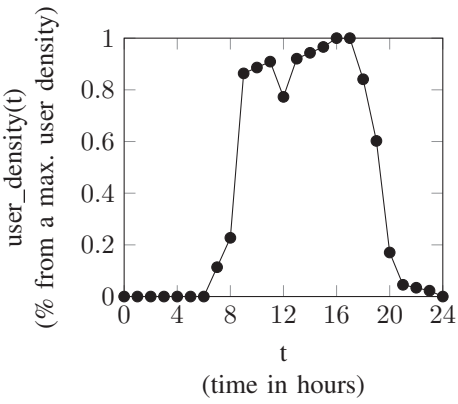

Fig. 4: User density as a percentile of the maximum user density per hour. Data source: [11]

III. Optimization Problem Formulation

The aim of the optimization is to maximize the total load that can be processed by the SBSs during T time steps. It is achieved by optimizing the on=1/off=0 statuses of all SBSs, which are described as Boolean variables $o_k^{(t)} \in \{0, 1\}$ for $t \in \{1, ..., T\}$ and $k \in \{1, ..., K\}$. A SBS serves every UE in its coverage area when it is on. A SBS does not serve any UE when it is off. Therefore the total load can be calculated as

$$R_k = \sum_{t=1}^{T} o_k^{(t)} l_k^{(t)} \tag{4}$$

All batteries have the same maximum battery capacity c_{max}. The battery levels in two successive time steps are linked through

$$\begin{aligned} &c_k^{(t)} = c_k^{(t-1)} + a_k^{(t-1)} - w_k^{(t-1)} - e_k^{(t-1)} \cdot o_k^{(t-1)} \\ &\forall t \in \{1, ..., T\} \text{ and } k \in \{1, ..., K\} \end{aligned} \tag{5}$$

where $c_k^{(t)}$ and $c_k^{(t-1)} (\in [0, c_{max}])$ donate the battery levels of the k^{th} SBS in the t^{th} and $(t-1)^{th}$ time steps, respectively, $a_k^{(t-1)}$ is the amount of harvested solar energy by the k^{th} SBS in the $(t-1)^{th}$ time step, $e_k^{(t-1)}$ and $w_k^{(t-1)}$ denote the energy consumption and the wasted energy due to battery overflow at the k^{th} SBS in the $(t-1)^{th}$ time step, respectively.

Let the vector $\boldsymbol{o_k} = \{o_k^{(1)}, o_k^{(2)}, \ldots, o_k^{(T)}\}$ denote the on/off statuses of the k^{th} SBS over T time steps. The optimization problem is formulated as follows.

$$\boldsymbol{o_k^*} = \text{ arg max}_{\boldsymbol{o_k}} R_k \tag{6}$$

subject to

$$\mathbf{0}^T \leq \boldsymbol{c_k^{(0)}}^T + \mathbf{M}_1 \cdot (\boldsymbol{a_k}^T - \boldsymbol{w_k}^T) - \mathbf{M}_k^{con} \cdot \boldsymbol{o_k}^T \leq \boldsymbol{c_{max}}^T \quad k \in \{1, ..., K\} \tag{7}$$

$$a_k^{(t)}, w_k^{(t)} \geq 0 \qquad \forall t \in \{1, ..., T\}, k \in \{1, ..., K\} \tag{8}$$

$$l_k^{(t)} \in \mathbb{N}_0 \qquad \forall t \in \{1, ..., T\}, k \in \{1, ..., K\} \tag{9}$$

$$o_k^{(t)} \in \{0, 1\} \qquad \forall t \in \{1, ..., T\}, k \in \{1, ..., K\} \tag{10}$$

$$0 \leq c_k^{(0)} \leq c^{max} \qquad k \in \{1, ..., K\} \tag{11}$$

where the vectors are of size T and are defined as $\boldsymbol{a_k} = \{a_k^{(1)}, a_k^{(2)}, \ldots, a_k^{(T)}\}$, $\mathbf{0} = \{\underbrace{0, \ldots, 0}_{T}\}$, $\boldsymbol{w_k} = \{w_k^{(1)}, w_k^{(2)}, \ldots, w_k^{(T)}\}$, and $\boldsymbol{c_k^{(0)}} = \{\underbrace{c_k^{(0)}, \ldots, c_k^{(0)}}_{T}\}$

and the two matrices $\mathbf{M}_1$ and $\mathbf{M}_k^{con}$ are of size TxT, with the element in the i^{th} row and the j^{th} column given by

$$\mathbf{M}_1(i,j) = \begin{cases} 1 & \text{if } i \geq j \\ 0 & \text{otherwise} \end{cases} \tag{12}$$

$$\mathbf{M}_k^{con}(i,j) = \begin{cases} e_k^{(j)} & \text{if } i \geq j \\ 0 & \text{otherwise} \end{cases} \tag{13}$$

Equation (7) insures that the battery level is kept within the range of $[0, c_{max}]$ in every time step. The $t^{th}(t \in \{1, ..., T\})$ row in $\mathbf{M}_1$ and $\mathbf{M}_k^{con}$ describes time step t. The t^{th} row of Equation (7) is obtained by recursively substituting (5) into $0 \leq c_k^{(t)} \leq c_{max}$ for t times. The values of $a_k^{(t)}$ and $l_k^{(t)}$ are input parameters to the optimization problem. As described in Subsection II-B and II-C, the values of $a_k^{(t)}$ can be derived from the database [10], and the values of $l_k^{(t)}$ are obtained from (3). Network operators can more reliably determine the values of $a_k^{(t)}$ by contacting the local met office and the values of $l_k^{(t)}$ by using their historical records of the local traffic load distribution.

IV. Numerical Analysis and Discussion

A. Cellular Network Setup

To evaluate the effects of different PV cell orientations on the performance of SBSs, we define three SBSs with three different orientation angles (east, south, and west orientated, respectively) but the same inclination angles, as given in TABLE I. The optimization problem (6) is then solved for the three SBSs separately. TABLE II shows the input parameters of the optimization problem (6) assuming that the SBS deployment is in London in December and June.

TABLE I: Orientation and inclination angles of the PV cells

	Orientation angle	Inclination angle
first SBS (east):	$-45°$	$38°$
second SBS (south):	$0°$	$38°$
third SBS (west):	$+45°$	$38°$

TABLE II: Input parameters for the optimization problem (6)

Parameter	Value
Time step period	15 minutes
e_{fix}	$34965J$
e_{user}	$80J$
c_{max}	$86400J$
$c_k^{(0)}$	$0J$
u_{max}	$471\frac{UE}{r_s^2\pi}$ with $r_s = 500$ metres
$a_k^{(t)}$	cf. (1) with $\eta = 0.15$
$l_k^{(t)}$	cf. (3)

B. Numerical Results

The optimization problem (6) is an integer optimization problem and can be solved using the simplex algorithm and the branch & bound method, which are available as an integer optimization solver in mathematical software packages such as MATLAB.

TABLE III: Percentage of UE which is served by the SBS during one day and which is offloaded to e.g. a grid connected MBS

	Percentage of UE served by the SBS	Percentage of UE offloaded to e.g. a grid connected MBS
December (east)	17.40%	82.60%
December (south)	20.60%	79.40%
December (west)	17.60%	82.40%
June (east)	65.76%	34.24%
June (south)	74.84%	25.16%
June (west)	80.34%	19.66%

	December			June				December			June		
Time	East	South	West	East	South	West	Time	East	South	West	East	South	West
00:00	0	0	0	0	0	0	12:00	1	1	0	1	1	1
00:15	0	0	0	0	0	0	12:15	0	0	0	1	1	1
00:30	0	0	0	0	0	0	12:30	0	1	1	1	1	1
00:45	0	0	0	0	0	0	12:45	0	0	0	1	1	1
01:00	0	0	0	0	0	0	13:00	1	0	1	1	1	1
01:15	0	0	0	0	0	0	13:15	0	1	0	1	1	1
01:30	0	0	0	0	0	0	13:30	1	1	1	1	1	1
01:45	0	0	0	0	0	0	13:45	0	0	0	1	1	1
02:00	0	0	0	0	0	0	14:00	0	0	0	1	1	1
02:15	0	0	0	0	0	0	14:15	0	0	1	1	1	1
02:30	0	0	0	0	0	0	14:30	0	1	0	1	1	1
02:45	0	0	0	0	0	0	14:45	0	0	0	0	1	1
03:00	0	0	0	0	0	0	15:00	0	0	0	1	1	1
03:15	0	0	0	0	0	0	15:15	0	0	0	0	1	1
03:30	0	0	0	0	0	0	15:30	0	0	0	1	1	1
03:45	0	0	0	0	0	0	15:45	0	0	0	0	0	1
04:00	0	0	0	0	0	0	16:00	0	0	0	1	1	1
04:15	0	0	0	0	0	0	16:15	0	0	0	0	1	1
04:30	0	0	0	0	0	0	16:30	0	0	0	0	0	1
04:45	0	0	0	0	0	0	16:45	0	0	0	1	1	1
05:00	0	0	0	0	0	0	17:00	0	0	0	0	0	0
05:15	0	0	0	0	0	0	17:15	0	0	0	0	1	1
05:30	0	0	0	0	0	0	17:30	1	0	1	0	0	1
05:45	0	0	0	0	0	0	17:45	0	0	0	1	0	0
06:00	0	0	0	0	0	0	18:00	0	0	0	0	0	1
06:15	0	0	0	0	0	0	18:15	0	0	0	0	1	0
06:30	0	0	0	0	0	0	18:30	0	0	0	0	0	0
06:45	0	0	0	1	0	0	18:45	0	0	0	0	0	1
07:00	0	0	0	1	1	1	19:00	0	0	0	0	0	0
07:15	0	0	0	1	1	1	19:15	0	0	0	0	0	0
07:30	0	0	0	1	1	1	19:30	0	0	0	0	0	0
07:45	0	0	0	1	1	0	19:45	0	1	0	1	1	0
08:00	0	0	0	1	1	1	20:00	0	0	0	0	0	0
08:15	0	0	0	1	1	1	20:15	0	0	0	0	0	0
08:30	0	0	0	1	1	1	20:30	0	0	0	0	0	0
08:45	0	0	0	1	1	1	20:45	0	0	0	0	0	0
09:00	0	0	0	1	1	1	21:00	0	0	0	0	0	1
09:15	0	0	0	1	1	0	21:15	0	0	0	0	0	0
09:30	1	0	0	1	1	1	21:30	0	0	0	0	0	0
09:45	0	1	0	1	1	1	21:45	0	0	0	0	0	0
10:00	0	0	0	1	1	1	22:00	0	0	0	0	0	0
10:15	1	1	1	1	1	1	22:15	0	0	0	0	0	0
10:30	0	0	0	1	1	1	22:30	0	0	0	0	0	0
10:45	0	0	0	1	1	1	22:45	0	0	0	0	0	0
11:00	1	1	0	1	1	1	23:00	0	0	0	0	0	0
11:15	1	0	1	1	1	1	23:15	0	0	0	0	0	0
11:30	0	1	0	1	1	1	23:30	0	0	0	0	0	0
11:45	0	0	1	1	1	1	23:45	0	0	0	0	0	0

Fig. 5: On/off status values of the simulated east, south and west orientated SBS in December and June

1) Comparison of the different orientations: The west/east orientated SBS is more likely to be on later/earlier in the day than the south orientated SBS in both months (cf. Fig. 5). This is caused by the solar energy profile output, which is shifted towards the evening/morning hours for the west/east orientated SBS compared to the southern SBS.

a) Comparison of the different orientations in winter: East and west orientated PV cells can serve 17.40% and 17.60% of their UEs, respectively, whereas the southern PV cell can serve with 20.60% the most UEs from all three different orientations in winter (cf. TABLE III). This is because the east and west orientated PV cell can generate less energy during this time of the year compared to the south orientated one due to their misalignment, therefore they can serve less UEs. The difference between the east and west SBS in TABLE III in winter is not significant enough and mainly caused by slightly better input values of the solar irradiance data sheet for the western PV cell from database [10] rather than the different orientation. Therefore both installations are considered to have the same performance in winter.

b) Comparison of the different orientations in summer: The situation is different during the summer month June, where the west orientated PV cell has the best performance and can serve 80.34% of its UEs (cf. TABLE III). This is caused by the shifted PV cell energy generation profile of the western PV cell towards the evening hours, which is similar to the traffic load profile. This proofs that the western orientation has a positive effect by adjusting the energy generation profile of the SBS to the consumption profile, so that less green energy is wasted due to less battery overflow. The second best performance in summer is achieved by the southern PV cell with 74.84%, followed by the eastern PV cell with 65.76% (cf. TABLE III).

2) Comparison of the different seasons: In general all PV cells serve more UEs during the summer than during winter due to their higher solar irradiance yield in this month (cf. TABLE III). The misalignment of the western and eastern PV cell in summer has not such a negative effect on the total energy generation of these PV cells throughout the day than in winter because the sun is higher up on the horizon in summer. Fig. 5 also proofs that all three SBSs are more likely to be on during summer because more solar energy is available in June.

3) Additional comments: It can be observed that for example the SBS (December (south)) is suddenly on again at 19:45 (cf. black arrow in Fig. 5), but there is not a lot of energy arriving at that time. This is due to the fact that the SBS has accumulated energy for many time steps so that there is sufficient energy available to serve UEs for one time step.

V. Conclusions

In this paper, we have investigated the effects of different orientated PV cells on the green energy utilization of a SBS. Our numerical results show that west orientated PV cells with $45°$ misalignment can serve more UEs throughout the day than a south or east ($45°$ misalignment) orientated one in London in summer. This contradicts the conventional assumption that the southern orientation of PV cells at SBSs is the optimal orientation on the northern hemisphere. It is therefore important to take into account the exact solar irradiance and traffic load pattern of the SBS's deployment site to determine which PV cell orientation should be chosen. On the one hand, countries with similar solar irradiance pattern as the UK during summer should deploy west orientated PV cells in business areas. On the other hand, countries with similar solar irradiance pattern as the UK during winter should deploy south orientated PV cells in business areas. In general, orientating PV cells to the east should be avoided because they reduce the green energy utilization of the SBS in all scenarios considered in this paper on the northern hemisphere.

REFERENCES

[1] Y. Wu, Y. Chen, J. Tang, D. K. C. So, Z. Xu, C. L. I., P. Ferrand, J. M. Gorce, C. H. Tang, P. R. Li, K. T. Feng, L. C. Wang, K. Borner, and L. Thiele, "Green transmission technologies for balancing the energy efficiency and spectrum efficiency trade-off," *IEEE Communications Magazine*, vol. 52, no. 11, pp. 112–120, Nov 2014.

[2] A. Kwasinski and A. Kwasinski, "Increasing sustainability and resiliency of cellular network infrastructure by harvesting renewable energy," *IEEE Communications Magazine*, vol. 53, no. 4, pp. 110–116, April 2015.

[3] Y. Mao, Y. Luo, J. Zhang, and K. B. Letaief, "Energy harvesting small cell networks: feasibility, deployment, and operation," *IEEE Communications Magazine*, vol. 53, no. 6, pp. 94–101, June 2015.

[4] G. Piro, M. Miozzo, G. Forte, N. Baldo, L. A. Grieco, G. Boggia, and P. Dini, "Hetnets powered by renewable energy sources: Sustainable next-generation cellular networks," *IEEE Internet Computing*, vol. 17, no. 1, pp. 32–39, Jan 2013.

[5] Y. Mao, Y. Luo, J. Zhang, and K. B. Letaief, "Energy harvesting small cell networks: feasibility, deployment, and operation," *IEEE Communications Magazine*, vol. 53, no. 6, pp. 94–101, June 2015.

[6] K. Huang, M. Kountouris, and V. O. K. Li, "Renewable powered cellular networks: Energy field modeling and network coverage," *IEEE Transactions on Wireless Communications*, vol. 14, no. 8, pp. 4234–4247, Aug 2015.

[7] H. Wang, H. Li, Z. Wang, X. Chen, and S. Ci, "Stochastic queue modeling and key design metrics analysis for solar energy powered cellular networks," in *Computing, Networking and Communications (ICNC), 2014 International Conference on*, Feb 2014, pp. 472–477.

[8] A. Luque and S. Hegedus, *Handbook of Photovoltaic Science and Engineering*, 2nd ed. John Wiley & Sons, 2011.

[9] M. A. Marsan, G. Bucalo, A. D. Caro, M. Meo, and Y. Zhang, "Towards zero grid electricity networking: Powering bss with renewable energy sources," in *2013 IEEE International Conference on Communications Workshops (ICC)*, June 2013, pp. 596–601.

[10] European Commission. (2016) Photovoltaic geographical information system (pvgis). [Online]. Available: http://re.jrc.ec.europa.eu/pvgis/

[11] CelPlan. (2014) White paper - customer experience optimization in wireless networks. [Online]. Available: http://www.celplan.com/resources/whitepapers/Customer%20Experience%20Optimization%20rev3.pdf